ChemComm

Controlling Carbodiimide-Driven Reaction Networks Through the Reversible Formation of Pyridine Adducts

Journal:	*ChemComm*
Manuscript ID	CC-COM-07-2024-003633.R1
Article Type:	Communication

ChemComm

COMMUNICATION

Controlling Carbodiimide-Driven Reaction Networks Through the Reversible Formation of Pyridine Adducts

Received 00th January 20xx,
Accepted 00th January 20xx

DOI: 10.1039/x0xx00000x

William S. Salvia, Georgia Mantel, Nirob K. Saha, Chamoni W. H. Rajawasam, Dominik Konkolewicz* and C. Scott Hartley*

Carbodiimides and pyridines form reversible adducts that slowly deliver carbodiimide "fuels" to out-of-equilibrium reaction networks, slowing activation kinetics and elongating transient state lifetimes. More-nucleophilic pyridines give more adduct under typical conditions. This approach can be used to extend the lifetimes of transient polymer hydrogels.

Responsive materials and molecular machines can be realized by non-equilibrium reaction networks operating through transient covalent bonds formed by "fueling" reactions.[1,2] Of many current options,[1–5] the hydration of carbodiimides is among the most useful.[6,7] These reaction networks usually function through the formation of transient aqueous carboxylic anhydrides generated by treating carboxylic acids with 1-ethyl-3-(3-dimethylaminopropyl)carbodiimide hydrochloride (EDC).[6–18] EDC is, however, arguably not a true carbodiimide—at typical pH it exists as a tautomeric guanidinium cation (Scheme 1a).[19] Conversely, 1-ethyl-3-(3-(dimethylamino)propyl)carbodiimide methiodide (mEDC), is analogous to EDC but unable to cyclize.[20] Consequently, mEDC is much more susceptible towards hydrolysis at most pHs (Table S1).[21]

Kinetic control underlies all nonequilibrium reaction networks, and thus controlling the rates of the component reactions is of critical importance. Substrate effects,[15] product phase separation,[10] and careful design of transient assemblies[16] can be used to control anhydride hydrolysis (deactivation) rates in carbodiimide-driven systems. Control over anhydride formation (activation) rates is so far restricted to the variation of the carbodiimide used.[6,17,22] Tunability is limited by the poor commercial availability of water-soluble carbodiimides.

Temporary deactivation of the carbodiimide is another possible way to tune its reactivity. Here, we show that mEDC reversibly forms adducts with pyridines that are inert to carboxylic acids, affording straightforward control over carbodiimide-driven reaction networks. By reducing the mEDC's effective concentration, the rate of anhydride formation is reduced. We find, in a simple model system and a transient polymer network hydrogel, that the adducts also act as reservoirs of carbodiimide to extend overall system lifetimes. Unlike prior examples that control the delivery of carboxylic acids by using anhydride[23,24] and ester[25] precursors, our reservoir operates on more-common carbodiimides and is generated reversibly in situ.

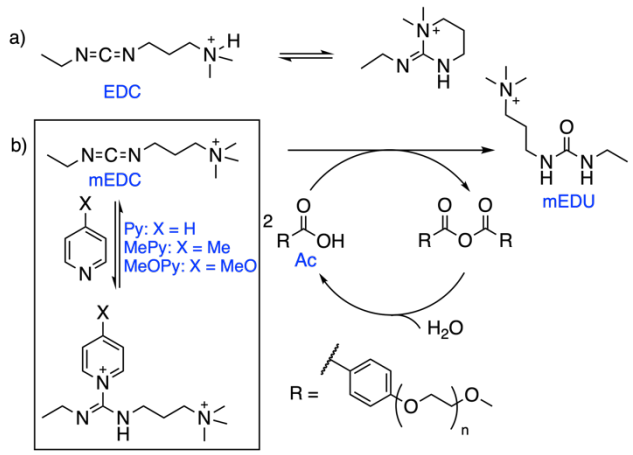

Scheme 1. (a) Ring-chain tautomerization of EDC and (b) adduct formation from mEDC coupled to transient anhydride formation. Avg. n = 11-12.

Pyridine (Py) is often added to carbodiimide-driven reaction networks, as a buffer, to inhibit the formation of undesirable *N*-acylurea byproducts,[14] and to shorten the lifetime of transient species to reasonable timescales.[15,18,26] When monitoring reactions of mEDC in the presence of Py, we noticed unexpected NMR signals that decayed over the course of the experiment. As shown in Figures 1 and S6-7, in the absence of carboxylic acid this new species forms immediately and then is lost at the same rate as the mEDC itself. We assigned the new species as the pyridine–mEDC adduct, formed as in Scheme 1b (box), based on NMR assignments (Figures S6-7) and MS (Figure S12). Note that nucleophilic attack on carbodiimides by amines, including triethylamine,[27] arylamines,[28] piperidine,[29] and imidazole,[29] is well-precedented (as is EDC's intramolecular cyclization, Scheme 1a[19]). However, in these cases the adducts are either

Department of Chemistry and Biochemistry, Miami University, 651 E. High St., Oxford, OH 45056, USA. E-mail: d.konkolewicz@miamioh.edu, scott.hartley@miamioh.edu

Supplementary Information available: [experimental details, kinetic data, kinetic simulations]. See DOI: 10.1039/x0xx00000x

unobserved reactive intermediates[27] or thermodynamically stable products.[28,29] Importantly, EDC itself does not form adducts with pyridine (Figure S11), presumably because of competition from its cyclization. The mEDC adduct concentration increased more than twofold when the Py concentration was increased from 100 to 300 mM (Figures 1, S40).

Pyridine itself gives a relatively low concentration of adduct; hence, we also tested more nucleophilic 4-methylpyridine (MePy) and 4-methoxypyridine (MeOPy).[30] To maximize the concentration of formed adduct, experiments were carried out at pD 5.5. As shown in Figures 1 and S40, adducts are formed when Py, MePy, or MeOPy are treated with an aqueous solution of mEDC, with higher adduct concentrations as pyridine nucleophilicity increases. Figure 1 compares the net mEDC available in the system (dashed black lines); with increasing adduct concentration, the overall consumption of mEDC is slower. For example, after ~20 min, about 40% of the MeOPy's total mEDC was consumed, compared to about 60% for Py.

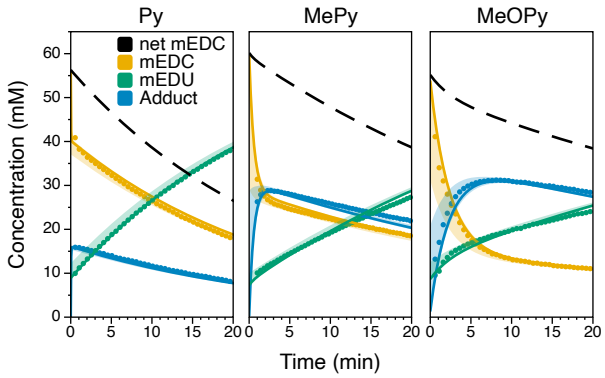

Figure 1. Change in concentrations over time for 300 mM Py, MePy, and MeOPy treated with 75 mM mEDC in D_2O at pD 5.5 and room temperature. The net mEDC (black, dashed) is the sum of the mEDC (orange) and adduct (blue) fits. Datapoints, fits, and 95% confidence intervals (shaded) are depicted for each species.

The concentration vs time plots for all three systems can be fit to a simple mechanism:[15]

$$\text{Carbodiimide} + \text{Pyridine} \underset{k_{-4}}{\overset{k_4}{\rightleftharpoons}} \text{Adduct} \quad (1)$$

$$\text{Carbodiimide} \xrightarrow{k_5} \text{Urea} \quad (2)$$

As expected, k_5 is indistinguishable with all three pyridines (Py: 5.3 × 10^{-2} min^{-1}, MePy: 4.4 × 10^{-2} min^{-1}, MeOPy: 4.8 × 10^{-2} min^{-1}). For Py, adduct formation (k_4) and decomposition (k_{-4}) are fast and thus only their ratio, K (k_4/k_{-4}), can be determined from our data. For MePy and MeOPy, these reactions are slower and k_4 and k_{-4} can be separately extracted (Table S2). The rate of formation (k_4) decreases in the order Py > MePy (3.0 M^{-1} min^{-1}) > MeOPy (0.92 M^{-1} min^{-1}). This can be justified by the more nucleophilic pyridines being deactivated by protonation at pD 5.5 (see Supporting Information). The rate of decomposition of the adduct (k_{-4}) follows the same trend, with Py > MePy (0.78 min^{-1}) > MeOPy (0.11 min^{-1}). That is, electron-donating groups stabilize the adduct. Despite the similar trends in k_4 and k_{-4}, the ratio K increases in the order Py (1.4 M^{-1}) < MePy (3.9 M^{-1}) < MeOPy (8.0 M^{-1}), and so more adduct accumulates for increasingly electron-donating substituents (Figure S86).[31]

To establish that adduct formation is orthogonal to carbodiimide-driven anhydride formation, and thus can both slow anhydride activation and establish an mEDC reservoir, we tested the complete reaction network in Scheme 1 using benzoic acid Ac as a simple model (avg. n = 11–12 in the polyethylene glycol chain).[7] Its anhydride was independently synthesized for reference (Figure S4).

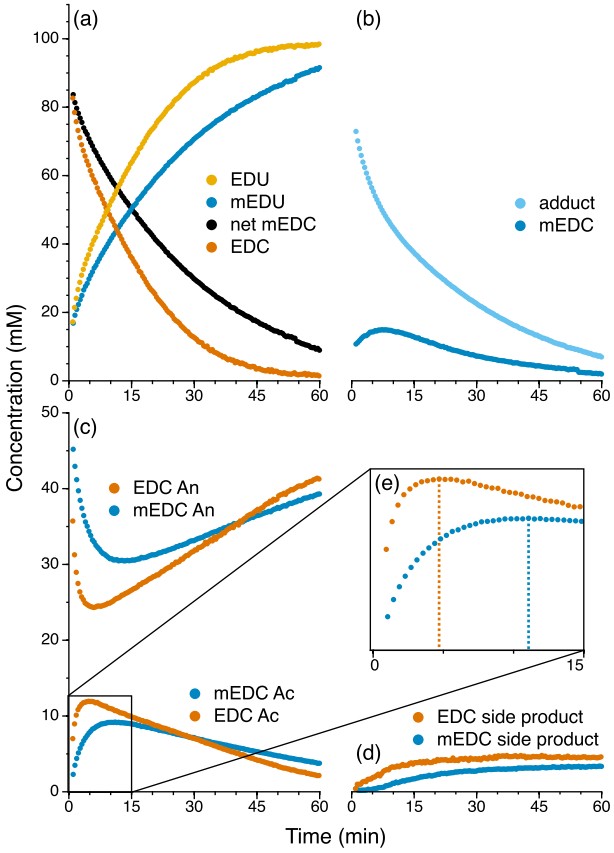

Figure 2. Changes in concentrations over time for 100 mM mEDC vs EDC in 300 mM MeOPy and 50 mM Ac with a 75 mM N,N-dimethylacetamide internal standard in D_2O at pD 5.5 and room temperature. An is the anhydride derived from Ac. The timescale is truncated for the mEDC experiment (see Figure S80). These experiments were scaled from raw ^1H NMR integral values. See pages S5-6 in Section 2 of the SI for further information.

Despite its slower on/off kinetics, MeOPy provides the highest concentration of adduct in the presence of Ac. In a typical experiment, MeOPy and mEDC were combined in D_2O and allowed to stand for 5 min to give time for the adduct to fully form. Without this premixing, the adduct concentration was much lower (Figure S76). This solution was then added to a solution of Ac. As a control, the reaction was carried out using EDC in place of mEDC, since EDC does not form the adduct. A control without MeOPy is not possible, since it affects other parts of the reaction network (e.g., catalyzing anhydride hydrolysis, see Eq 3-7, Figures S77-78) and acts as the buffer.

Notably, in the mEDC sample, when compared to the EDC sample, there was a substantial decrease in the rate of formation of the anhydride (Figure 2e) and the lifetime was

longer (Figure 2c). With mEDC, the anhydride reached its peak concentration at 11 min, compared to 4.7 min for EDC, a 134% increase, which resulted in a 17% decrease in peak anhydride concentration as anhydride formation competed less effectively with hydrolysis. Further, the mEDC is lost more slowly than the EDC, despite mEDC's increased hydrolysis rate, as shown by comparing Figure 2a's "net mEDC" curve, the sum of the curves in Figure 2b, with Figure 2a's "EDC" curve (though, surprisingly, EDC and mEDC were found to have the same reactivity towards Ac, Table S1). The concentration of free mEDC was consistently low (<15 mM) but it was continuously released from the adduct, as shown in Figure 2b. The anhydride therefore persisted longer for mEDC relative to the EDC because the adduct acts as a carbodiimide reservoir. The lifetimes, defined as the time taken for the Ac to return to 80% of its original value, were 63 min and 54 min for mEDC and EDC, respectively, an approximately 20% increase. The magnitude of lifetime extension is complicated by the presence of the adduct, which decreases the concentration of pyridine available for anhydride hydrolysis catalysis, although this effect cannot by itself account for the difference in lifetime (see Supporting Information).

A small amount of a side product was found in both the EDC (4.6 mM) and mEDC (3.4 mM) systems (Figure 2d). It is longer-lived than the anhydride but transient, decomposing back to Ac over the course of days (Figure S84). Despite significant efforts, we have been unable to conclusively identify this compound. Our current working hypothesis is that it is derived from the reaction of water with the acylpyridinium intermediate (Figure S85, Scheme S3).

Adduct formation behaves similarly with another carboxylic acid, 4-sulfobenzoic acid monopotassium salt (KSBA). A similar side product was also observed with KSBA (Figure S79).

The mechanism in Eq 3–8, assuming a steady-state in the acylpyridinium ($\alpha = k_2/k_3$) and that $k_{fast} >> k_1$, successfully fits the data for all three pyridines (see Eq S13–S27):

$$\text{Acid} + \text{Carbodiimide} \xrightarrow{k_1} \textit{O}\text{-Acylisourea} \quad (3)$$

$$\textit{O}\text{-Acylisourea} + \text{Pyridine} \xrightarrow{k_{fast}} \text{Acylpyridinium} + \text{Urea} \quad (4)$$

$$\text{Acylpyridinium} + \text{Acid} \underset{k_{-2}}{\overset{k_2}{\rightleftharpoons}} \text{Anhydride} + \text{Pyridine} \quad (5)$$

$$\text{Acylpyridinium} \xrightarrow{k_3} \text{Acid} + \text{Pyridine} \quad (6)$$

$$\text{Carbodiimide} + \text{Pyridine} \underset{k_{-4}}{\overset{k_4}{\rightleftharpoons}} \text{Adduct} \quad (7)$$

$$\text{Carbodiimide} \xrightarrow{k_5} \text{Urea} \quad (8)$$

Note that, because of its low concentration, the side product was not included in the mechanism. Unfortunately, the parameters α and k_{-2} are correlated in these fits and cannot be determined from the experimental data alone. That is, the model cannot determine whether anhydride both forms and decomposes quickly or slowly. However, Ferscht and Jencks have reported values k_{-2} for the hydrolysis of acetic anhydride by Py, MePy, and MeOPy, which we can use to determine the general substituent effect on α (Table S4).[32] This previous work suggests that the parameter k_{-2} (Eq 5) increases from Py to MePy to MeOPy, meaning that more electron-rich pyridines attack more quickly. While acetic anhydride undergoes hydrolysis much faster than the benzoic-acid-derived anhydride from Ac,[33] the trend likely holds. In the present work, this suggests that α is independent of the type of pyridine used (Table S4). Thus, as more nucleophilic pyridines are used, the increased value of k_{-2} leads to faster breakdown and decreased concentration of the anhydride, both when the adduct is present and absent (Figures S81-82, Table S4).

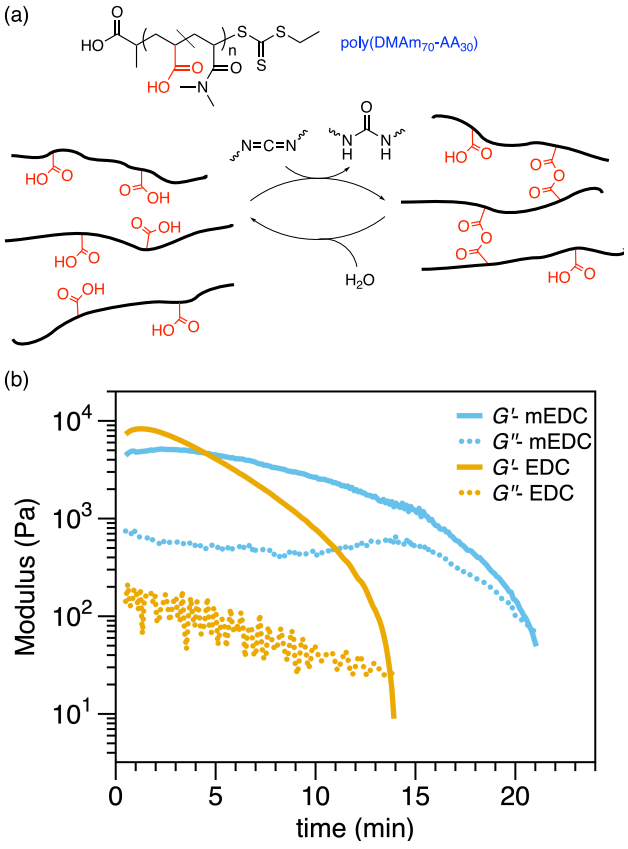

Figure 3. a) Transient hydrogel formation from poly($DMAm_{70}$-AA_{30}). b) Storage (G', solid) and loss (G'', dashed) moduli over time for mEDC (blue) and EDC (orange).

To establish that mEDC–pyridine adducts can affect the behavior of a functional system, the carbodiimide-driven crosslinking of poly($DMAm_{70}$-AA_{30}), shown in Figure 3a, was used as a model. On treatment with carbodiimide, a solution of poly($DMAm_{70}$-AA_{30}) forms a polymer network hydrogel through the generation of anhydride crosslinks from the pendant carboxylic acid groups.[3] The gel eventually returns to a liquid state as the anhydride linkages hydrolyze. To test the effect of adduct formation, 500 mM of mEDC and 100 mM MeOPy were added to an aqueous solution of poly($DMAm_{70}$-AA_{30}). This provides an initial 400 mM of free carbodiimide to initiate gelation (determined from preliminary experiments) along with an additional 100 mM to serve as a reservoir through the formation of adduct. As before, the MeOPy and mEDC were premixed for 5 min before addition to the hydrogel to allow the adduct concentration to peak.

Figure 3b shows the rheological time sweep data for gelation and degelation of poly(DMAm$_{70}$-AA$_{30}$). As before, EDC was used as a control as it does not form an adduct with MeOPy. On addition of carbodiimide, both systems underwent rapid gelation, as indicated by storage moduli (*G*') greater than loss moduli (*G*"). With mEDC, the peak *G*', which corresponds to the peak anhydride crosslink density, occurred at 130 s, compared to 70 s with for EDC, an 86% increase. The peak *G*' was also noticeably lower for mEDC compared to EDC. Similarly, the hydrogel had a substantially longer 20 min lifetime with mEDC, compared to 14 min for EDC, a 43% increase. These results are consistent with the effects of adduct formation in the mEDC system. The delayed and lower peak *G*' implies a slower activation rate compared to EDC because the concentration of free carbodiimide is lower early in the experiment, in line with the results from the Ac system. Similarly, the longer lifetime is consistent with slowly released carbodiimide from the adduct over an extended period, giving an extended plateau of *G*'.

In summary, the formation of carbodiimide–pyridine adducts from mEDC is orthogonal to carbodiimide-driven anhydride formation. Pyridine additives therefore control the availability of carbodiimide, decreasing activation rates and prolonging anhydride lifetimes beyond those of EDC. In a transient hydrogel as a representative functional material, the time to peak modulus increased by 86% and the lifetime was extended by 43% for an mEDC/4-methoxypyridine system compared to the EDC control. This strategy provides additional tuning of the kinetics of carbodiimide-driven chemical systems by expanding the reaction network.

Conflicts of interest

There are no conflicts to declare.

Acknowledgements

This work was supported by United States Department of Energy, Office of Science, Basic Energy Sciences, under Award No. DE-SC0018645.

Data availability

Data for this article, including kinetic and NMR data are available at Miami University Scholarly Commons at http://hdl.handle.net/2374.MIA/6979.

Notes and references

1 J. Boekhoven, W. E. Hendriksen, G. J. M. Koper, R. Eelkema and J. H. van Esch, *Science*, 2015, **349**, 1075–1079.
2 M. R. Wilson, J. Solà, A. Carlone, S. M. Goldup, N. Lebrasseur and D. A. Leigh, *Nature*, 2016, **534**, 235–240.
3 O. J. Dodo, L. Petit, C. W. H. Rajawasam, C. S. Hartley and D. Konkolewicz, *Macromolecules*, 2021, **54**, 9860–9867.
4 W. A. Ogden and Z. Guan, *ChemSystemsChem*, 2020, **2**, e1900030.
5 D. Del Giudice and S. Di Stefano, *Acc. Chem. Res.*, 2023, **56**, 889–899.
6 M. Tena-Solsona, B. Rieß, R. K. Grötsch, F. C. Löhrer, C. Wanzke, B. Käsdorf, A. R. Bausch, P. Müller-Buschbaum, O. Lieleg and J. Boekhoven, *Nat. Commun.*, 2017, **8**, 15895.
7 L. S. Kariyawasam and C. S. Hartley, *J. Am. Chem. Soc.*, 2017, **139**, 11949–11955.
8 S. Bai, X. Niu, H. Wang, L. Wei, L. Liu, X. Liu, R. Eelkema, X. Guo, J. H. van Esch and Y. Wang, *Chem. Eng. J.*, 2021, **414**, 128877.
9 C. W. H. Rajawasam, C. Tran, M. Weeks, K. S. McCoy, R. Ross-Shannon, O. J. Dodo, J. L. Sparks, C. S. Hartley and D. Konkolewicz, *J. Am. Chem. Soc.*, 2023, **145**, 5553–5560.
10 C. Donau and J. Boekhoven, *Trends Chem.*, 2023, **5**, 45–60.
11 M. M. Hossain, I. M. Jayalath, R. Baral and C. S. Hartley, *ChemSystemsChem*, 2022, **4**, e202200016.
12 S. Mondal and D. Haldar, *New J. Chem.*, 2021, **45**, 4773–4779.
13 M. Cheng, C. Qian, Y. Ding, Y. Chen, T. Xiao, X. Lu, J. Jiang and L. Wang, *ACS Mater. Lett.*, 2020, **2**, 425–429.
14 X. Chen, H. Soria-Carrera, O. Zozulia and J. Boekhoven, *Chem. Sci.*, 2023, **14**, 12653–12660.
15 L. S. Kariyawasam, J. C. Kron, R. Jiang, A. J. Sommer and C. S. Hartley, *J. Org. Chem.*, 2020, **85**, 682–690.
16 S. Bal, K. Das, S. Ahmed and D. Das, *Angew. Chem. Int. Ed.*, 2019, **58**, 244–247.
17 B. A. K. Kriebisch, A. Jussupow, A. M. Bergmann, F. Kohler, H. Dietz, V. R. I. Kaila and J. Boekhoven, *J. Am. Chem. Soc.*, 2020, **142**, 20837–20844.
18 A. Englert, F. Majer, J. L. Schiessl, A. J. C. Kuehne and M. von Delius, *Chem*, 2024, **10**, 910–923.
19 I. T. Ibrahim and A. Williams, *J. Am. Chem. Soc.*, 1978, **100**, 7420–7421.
20 T. Tenforde, R. A. Fawwaz, N. K. Freeman and N. Jr. Castagnoli, *J. Org. Chem.*, 1972, **37**, 3372–3374.
21 A. Williams and I. T. Ibrahim, *J. Am. Chem. Soc.*, 1981, **103**, 7090–7095.
22 S. Borsley, D. A. Leigh, B. M. W. Roberts and I. J. Vitorica-Yrezabal, *J. Am. Chem. Soc.*, 2022, **144**, 17241–17248.
23 C. Biagini, G. Capocasa, D. Del Giudice, V. Cataldi, L. Mandolini and S. Di Stefano, *Org. Biomol. Chem.*, 2020, **18**, 3867–3873.
24 C. Biagini, G. Capocasa, V. Cataldi, D. Del Giudice, L. Mandolini and S. Di Stefano, *Chem. – Eur. J.*, 2019, **25**, 15205–15211.
25 T. Heuser, A.-K. Steppert, C. Molano Lopez, B. Zhu and A. Walther, *Nano Lett.*, 2015, **15**, 2213–2219.
26 X. Chen, M. Stasi, J. Rodon-Fores, P. F. Großmann, A. M. Bergmann, K. Dai, M. Tena-Solsona, B. Rieger and J. Boekhoven, *J. Am. Chem. Soc.*, 2023, **145**, 6880–6887.
27 M. V. Vovk, P. S. Lebed', A. N. Chernega and V. V. Pirozhenko, *Russ. J. Org. Chem.*, 2002, **40**, 195–198.
28 J. Bhattacharjee, A. Harinath, I. Banerjee, H. P. Nayek and T. K. Panda, *Inorg. Chem.*, 2018, **57**, 12610–12623.
29 T.-H. Zhu, S.-Y. Wang, Y.-Q. Tao and S.-J. Ji, *Org. Lett.*, 2015, **17**, 1974–1977.
30 DMAP and 4-chloropyridine were also tested; neither give adduct.
31 Corwin. Hansch, A. Leo and R. W. Taft, *Chem. Rev.*, 1991, **91**, 165–195.
32 A. R. Fersht and W. P. Jencks, *J. Am. Chem. Soc.*, 1970, **92**, 5432–5442.
33 C. A. Bunton and S. G. Perry, *J. Chem. Soc.*, 1960, 3070–3079.

Data Availability Statement: Controlling Carbodiimide-Driven Reaction Networks Through the Reversible Formation of Pyridine Adducts

Data for this article, including kinetic and NMR data are available at Miami University Scholarly Commons at http://hdl.handle.net/2374.MIA/6979 .